Up-scalable method to amplify the diffraction efficiency of simple gratings

Fabian Lütolf,[1,2,]* Martin Stalder,[2] and Olivier J. F. Martin[1]

[1]*Nanophotonics and Metrology Laboratory, Swiss Federal Institute of Technology Lausanne, Lausanne CH-1015, Switzerland*

[2]*CSEM Centre Suisse d' Electronique et de Microtechnique, Tramstrasse 99 Muttenz CH-4132, Switzerland*

*Corresponding author: fabian.luetolf@epfl.ch

An innovative class of coupling gratings for efficiently redirecting light beams is described. They are based on symmetric binary gratings equipped with an asymmetric high refractive index coating. This kind of structure exhibits a grating blaze effect and produces high diffraction efficiencies. Coupling gratings based on the described principle have been fabricated by UV casting and subsequent oblique ZnS evaporation. The gratings were characterized by measuring their diffraction efficiencies. For unpolarized light, efficiencies of around 70% have been measured at 510 nm wavelength. Simulations revealed that diffraction efficiencies of up to 90% can be obtained for polarized light. © 2014 Optical Society of America

OCIS codes: (050.1950) Diffraction gratings; (310.1860) Deposition and fabrication.

http://dx.doi.org/10.1364/OL.39.006557

Gratings are key building blocks for applied optics since many optical systems such as photospectrometric instruments, lasers, solar concentrators/cells [1], waveguides [2], or sensors [3] rely on the efficient and selective redirection of light. Metallic gratings further allow the excitation of surface plasmons [4], which open up many interesting applications in optics [5]. The standard approach to redirect light by diffraction is to use asymmetric gratings such as sawtooth, slanted [6], subperiod binary blazed [7] or multilevel blazed gratings [8] since they are capable of diffracting the light more efficiently. This is especially true for normally incident light and one preferred diffraction order. Unfortunately, all of the previously mentioned gratings are either challenging to fabricate (sawtooth, binary blazed, and staircase blazed gratings) or to replicate (slanted gratings and binary blazed gratings).

In this Letter, we present an original approach to fabricating asymmetric diffractive gratings, which does not require sophisticated grating masters. Readily available binary gratings are replicated in a standard UV casting process and subsequently angle evaporated with either dielectrics or metals, to blaze the grating replica. This simple yet powerful procedure was already used more than 30 years ago to generate structures as small as ≈10 nm [9]. We use the same technique to apply a ZnS coating and achieve unpolarized first diffraction order transmittance (T1) efficiencies at perpendicular incidence close to 70%. All the processes are suitable for mass production, and therefore this approach is a flexible alternative to existing procedures for industrial manufacturing of blazed gratings. Since the grating is very simple, it can be replicated by any of the common mass production methods such as hot embossing or injection molding, and is not limited to UV casting. Finally, the structure remains functional even when embedded in the substrate material, which is not the case when using any embossed surface relief grating (similar to buried high refractive index coatings recently investigated [10]).

Figure 1 illustrates the fabrication procedure: a UV curable polymer is casted against a nickel master grating with 440 nm period, Fig. 1(a). Subsequently, 150 nm of ZnS are evaporated on the grating at an angle using a Balzers BAE 250 coating system, Fig. 1(b). ZnS has a high and well controlled refractive index. An SEM picture of the resulting asymmetric structure, produced by self-shadowing of the grating, is shown in Fig. 1(c). We have also investigated metallic coatings, starting with a 440 nm period grating with subsequent evaporation of 20 nm Al at an angle $\alpha < 70°$ with respect to the surface normal in a Balzers BAK 550 system. The latter structure is shown in the inset of Fig. 4. Note that the coating can be tuned by varying the evaporation angle or the distance between sample and source material. (This determines, for example, the coating thickness on the shadowed sidewall.)

To understand the response of such gratings, we have performed numerical simulations using rigorous-coupled-wave analysis (RCWA) based programs [11]. The model used for these simulations is sketched in Fig. 1(d). Figure 1(b) additionally shows the definition of polarizations (TE and TM) for a grating in classical mount, which is also commonly used at perpendicular
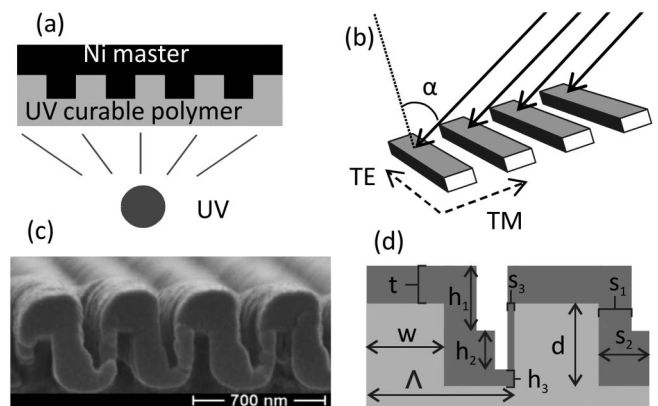
Fig. 1. (a) and (b) Fabrication procedure and orientation of the E-vector with respect to the grating for the two polarizations, (c) SEM picture of the obtained structure, and (d) model used for simulations.
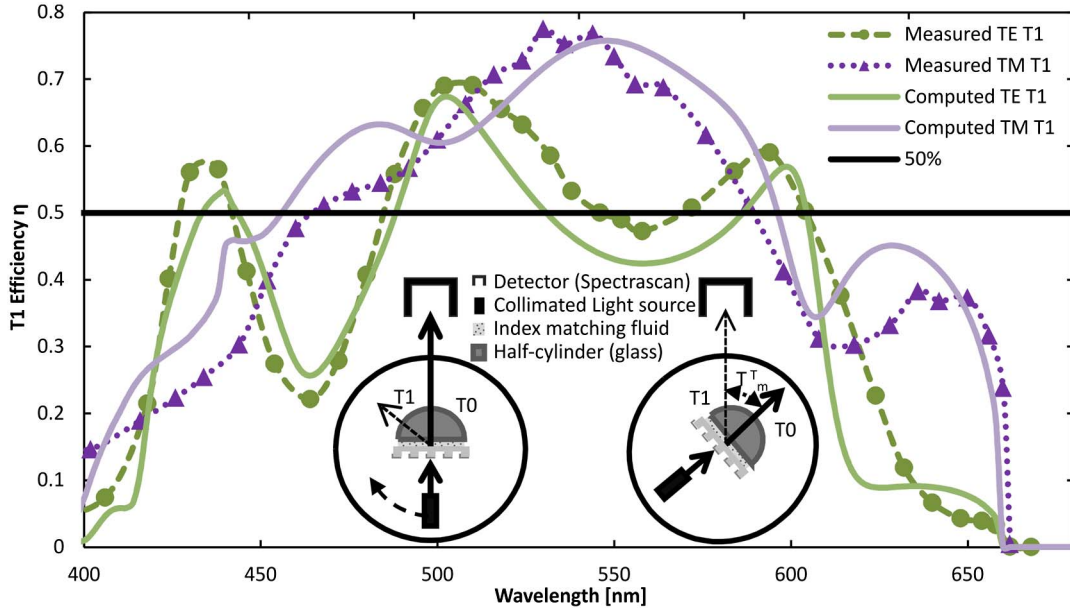
Fig. 2.   Maxima of the measured first-order diffraction efficiencies (filled symbols) for both polarizations at perpendicular incidence, together with the corresponding computed data (solid lines). Those results were obtained with the structure shown in Fig. 1(c). Inset: sketch of the measurement setup and how it allows measuring T0 and T1 at angles between 0° and 80°.

incidence as chosen in the present simulations and experiments.

Next we have carried out measurements of the diffraction efficiency (η) of light into T1 for such prepared gratings. T1 measurements were performed using the setup sketched in the inset of Fig. 2: white light from a DH-2000 tungsten lamp (Ocean Optics) impinges perpendicularly on the grating. A half-cylindrical lens with radius approximately equal to lens thickness, plus the substrate thickness, was mounted on the back of the substrate with index matching fluid to prevent total internal reflection and preserve the coupling angles Θ_m^T for the measurements. The whole setup was mounted on a rotating plate, allowing the configuration to remain stable while the diffracted light is measured at the given angles. This diffracted light was collected with a PR-705 Spectrascan Spectroradiometer at angles Θ_1^T between 36° and 84° in steps of 2°. The resulting spectra were divided by the intensities measured through an unstructured part of the glass sample in order to normalize the data. The gray curves in Fig. 4 serve as examples. In Figs. 2 and 4, only the maxima measured for the different angles are shown (filled symbols and crosses respectively).

The calculation of the diffraction angles Θ_m^T for any wavelength can be performed using Eq. (1):

$$\theta_m^T = \sin^{-1}\left(\frac{n_1 \sin \theta_i + m\frac{\lambda}{\Lambda}}{n_2}\right), \qquad (1)$$

where n_1 is the refractive index of the surrounding material, n_2 the refractive index of the substrate material, Θ_i the angle of incidence, m the diffraction order, Λ the grating period, and λ the vacuum wavelength.

At perpendicular incidence ($\Theta_i = 0$), for most of the visible spectrum, only T0, T1, and $T-1$ exist for the grating under study with a $\Lambda = 440$ nm period: for $m = \pm 1$ and $n_2 = 1.5$, wavelengths up to $\lambda = 660$ nm are

diffracted, whereas the maximum diffraction wavelength for $m = \pm 2$ lies at $\lambda = 330$ nm. The angles for the first reflection diffraction orders $R \pm 1$ are obtained by choosing $n_2 = 1$, which yields a maximum wavelength of $\lambda = 440$ nm for the same grating. These calculations motivate the choice of $\Lambda = 440$ nm as the preferred grating period: no transmission orders above 1 and no reflection orders apart from 0 exist in the visible, thus allowing for maximum T1. Additionally, at perpendicular incidence, all wavelengths between 440 and 660 nm are diffracted to angles larger than the total internal reflection angle, therefore allowing for waveguide coupling of almost the entire visible spectrum.

The corresponding simulation model is shown in Fig. 1(d). The refractive index was set to 1.5 for the substrate (polymer/glass) and to 1 for the top material (air). Refractive index data for ZnS is obtained from [12]. The geometrical parameters are $t = 150$ nm, $w = 0.33\Lambda$, $d = 285$ nm (the shrinkage coming from heat transfer during evaporation), $h_2 = 0.66 * t$, $h_3 = 0.37 * t$, $h_1 = t + d - h_1 - h_2$, $s_1 = 0.66 * t$, $s_2 = 1.15 * t$, and $s_3 = 0.15 * t$, which is consistent with SEM measurements. The simulation results are plotted with the measurements (hollow symbols in Fig. 2). The agreement between simulations and measurements is very good for both polarizations.

The measurements in Fig. 2 show first-order transmittance efficiencies (T1) of almost 70% (neglecting the $\approx 4\%$ reflectance off the reference glass) for both polarizations simultaneously at around $\lambda = 510$ nm (green). Note that this is well above the theoretical limit of $<50\%$ T1 for a symmetric grating at perpendicular incidence, clearly demonstrating the strong enhancement of the T1 efficiency caused by the asymmetric coating. T–1 will not be considered since it is very low by design.

The effect of the asymmetric coating on the bare binary grating is also visualized in the following series of simulations (Fig. 3) that show how T1 efficiencies
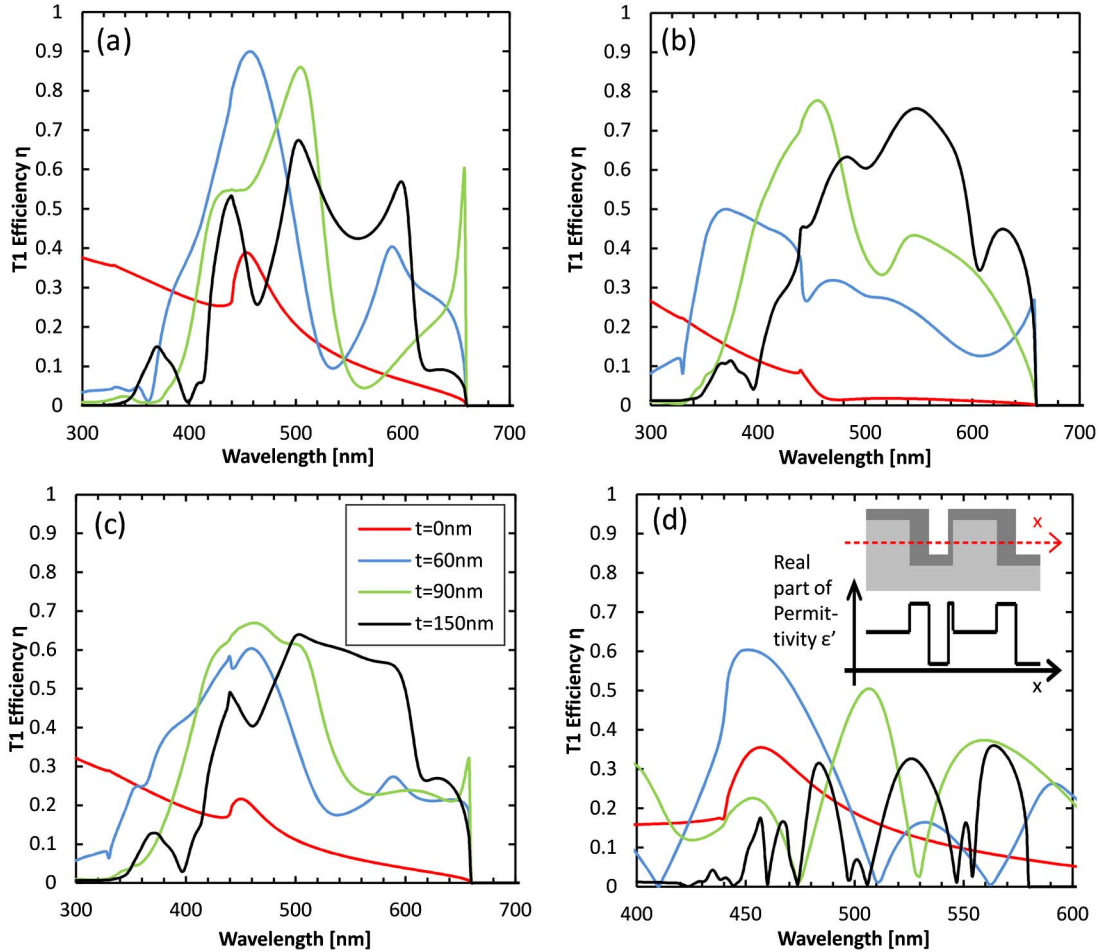
Fig. 3.   Computed T1 data is plotted for increasing ZnS thicknesses t for (a) TE polarized light and (b) TM polarized light. (c) The average of the two is shown, and (d) the difference between them is shown. Inset: schematic representation of the real part of the permittivity (black line) at the lateral position indicated by the red axis in the structure sketched above.

evolve by increasing the ZnS coating thickness t from 0 to 150 nm. A common trend seen for all the gratings and coatings investigated is that by increasing the coating thickness, T1 is first enhanced for TE polarized light [peaking at $\eta = 90\%$ for 60 nm of ZnS in the present case, Fig. 3(a)], whereas efficient diffraction of TM polarized light requires thicker coating layers [peaking at $\eta = 80\%$ efficiency for 120 nm of ZnS, data not shown. This finding is consistent with the general design rule $d + t = \lambda/(n - 1)$ for 2π phase shift modulators as, for example, used for binary blazed gratings [7]. For $h = 90$ nm, $t = 285$ nm, and $n = 2.4$ we receive $\lambda = 525$ nm, which is close to the maximum of the green curve in Fig. 3(a). It is also well understood that, in 1D gratings, the effective refractive index is lower for TM polarized light than for TE polarized light [13], which explains the discrepancy between the two maxima.

The simulations also show that by increasing the ZnS thickness, spectral features of T1 not only increase in intensity before diminishing again, but also demonstrate additional peaks in the blue portion of the spectrum and then red shift until they reach wavelengths that are evanescent [Θ_m^T in Eq. (1) becomes 90°, which occurs at $\lambda = 660$ nm for the grating considered here]. Since the peaks for TE and TM polarized light are not spectrally

aligned, intersections of the two curves provide the wavelengths for unpolarized operation.

To this end, Fig. 3(d) shows the absolute value of the T1 intensity difference between both polarizations, which should be as low as possible to keep the coupled light unpolarized. For green light, where the human eye is the most sensitive, the 150 nm ZnS coating fulfills this requirement best [black line in Fig. 3(d)]. Therefore, although in the relevant wavelength range, other ZnS coatings would provide slightly higher total diffraction efficiency blue line in Fig. 3(c) than 150 nm, the thicker coating was chosen for the present device.

The present structure can be related to multilevel blazed gratings when looking at the cross section perpendicular to the grating lines. The inset in Fig. 3 illustrates qualitatively how the real part of permittivity varies along the x axis (indicated in red) through the cross section. The shape of the resulting graph looks similar to the cross section of a multilevel blazed grating [8], which provides an explanation for the blazed behavior.

In addition to dielectric coatings, this approach was also used for the evaporation of metals. Metals like silver, gold, or aluminum have refractive indices between 0.1 and 1.5 in the visible, but exhibit high absorption coefficients k. This results in a strongly negative real part of the
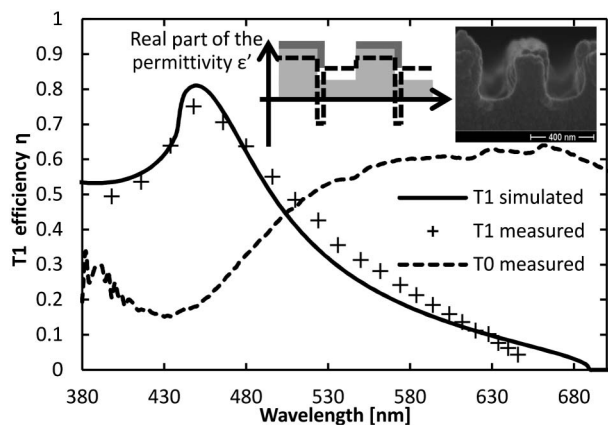
Fig. 4. Experimental T1 efficiencies (crosses) measured for perpendicularly incident TE polarized light at the individual angles plotted together with the computed data (black solid line) and zero order transmittance (dotted line). The graph exhibits efficiencies in excess of 70% for the metalized grating shown in the SEM image of the inset. The inset also depicts the real part of the permittivity along the cross section of such a structure.

permittivity $\varepsilon' = n^2 - k^2$, and therefore in a high absolute difference between the substrate and the metals' permittivities.

This difference is much higher for metals ($\varepsilon' \approx -35$, resulting in a difference of $\Delta\varepsilon' \approx -37$ in the case of aluminum [14]) than for high refractive index materials such as ZnS ($\varepsilon' \approx 6.75$, resulting in a difference of $\Delta\varepsilon' \approx 4.5$). Very thin metal coatings (5–20 nm) can already strongly enhance T1 efficiencies: Fig. 4 illustrates how T1 efficiencies in excess of 70% can be achieved for TE polarized light when using angle evaporation of 20 nm aluminum. Simulations using a model based on the SEM image were performed to verify this finding (solid line in Fig. 4).

Additional simulations were performed in search of an explanation for this effect. We substituted the refractive index of the Al coating with an artificial material with a constant complex index of refraction of $n = 1$ (matching the superstrate's index) and $k = 5.4$, and could reproduce the strong enhancement of T1 also for the artificial material.

This observation suggests that the parameter to consider when tuning coatings for increasing diffraction efficiencies is indeed the real part of permittivity and not the refractive index n. The inset in Fig. 4 illustrates qualitatively how the permittivity of the structure changes along the metallized grating's cross section, which is again very similar to the cross section of a multilevel blazed grating [8]. The same explanation previously used for dielectric coatings therefore also holds for the enhanced T1 efficiency observed for metallized gratings.

Thicker metal coatings appear to strongly enhance reflection into a single higher order (computed data not shown). For TM polarized light and properly chosen parameters, the present structure might also be capable of enhancing one of the evanescent modes to launch surface plasmons into a specific direction (similar to already investigated asymmetric metal gratings [15]). However, a general drawback of using metals for light diffraction is the inherent absorption (as evident from the non-zero imaginary part of the permittivity ε_2).

The asymmetric dielectric structure can also be embedded into the substrate polymer, for example, while still providing diffraction efficiencies in excess of 50% at perpendicular incidence (simulation data not shown). This property allows protecting the active structure from wear and other environmental influences such as humidity or, in the case of metals, oxidation.

In conclusion, efficient first-order transmittance coupling was shown on simple, symmetric basic gratings, asymmetrically coated with a high refractive index dielectric material or metal. For a fabricated structure optimized for unpolarized light, around 70% of the perpendicularly incoming light was diffracted into T1 according to our measurements. Standard replication techniques such as hot embossing or UV casting can be used to duplicate a basic grating, which can subsequently be coated at oblique incidence with either a high refractive index material or a metal. Another important property of such a structure is that it retains its high efficiency independently of the refractive index of a possible cladding layer. Laminating or embedding the structure will protect it from wear and make it well suited for applications in harsh conditions. Finally, all the different methods used here are well suited for roll-to-roll manufacturing or other high throughput processes.

References

1. V. Gate, Y. Jourlin, M. Langlet, F. Vocanson, O. Parriaux, G. Bernaud, C. Veillas, and A. Cazier, Proc. SPIE **8438**, 84380W (2012).
2. N. Destouches, D. Blanc, J. Franc, S. Tonchev, N. Hendrickx, P. Van Daele, and O. Parriaux, Opt. Express **15**, 16870 (2007).
3. L. Davoine, V. Paeder, G. Basset, M. Schnieper, and H. P. Herzig, Appl. Opt. **52**, 340 (2013).
4. T. W. Ebbesen, H. J. Lezec, H. F. Ghaemi, T. Thio, and P. A. Wolff, Nature **391**, 667 (1998).
5. B. Gallinet, T. Siegfried, H. Sigg, P. Nordlander, and O. J. F. Martin, Nano Lett. **13**, 497 (2013).
6. J. M. Miller, N. de Beaucoudrey, P. Chavel, J. Turunen, and E. Cambril, Appl. Opt. **36**, 5717 (1997).
7. S. Astilean, P. Lalanne, P. Chavel, E. Cambril, and H. Launois, Opt. Lett. **23**, 552 (1998).
8. M. Oliva, D. Michaelis, F. Fuchs, A. Tünnermann, and U. D. Zeitner, Appl. Phys. Lett. **102**, 203114 (2013).
9. D. Flanders and A. White, J. Vac. Sci. Technol. **19**, 892 (1981).
10. R. Bruck and R. Hainberger, Appl. Opt. **49**, 1972 (2010).
11. M. G. Moharam and T. K. Gaylord, J. Opt. Soc. Am. **71**, 811 (1981).
12. M. Bass, C. DeCusatis, J. Enoch, V. Lakshminarayanan, G. Li, C. MacDonald, V. Mahajan, and E. V. Stryland, *Handbook of Optics, Third Edition Volume IV: Optical Properties of Materials, Nonlinear Optics, Quantum Optics (set)* (McGraw-Hill2009).
13. D. C. Flanders, Appl. Phys. Lett. **42**, 492 (1983).
14. A. Rakic, Appl. Opt. **34**, 4755 (1995).
15. B. Bai, X. Meng, J. Laukkanen, T. Sfez, L. Yu, W. Nakagawa, H. P. Herzig, L. Li, and J. Turunen, Phys. Rev. B **80**, 035407 (2009).